A Different Approach to Vent Flow Calculations in Fire Compartments using the Critical Flow Condition

GEORGES GUIGAY,* JÓNAS ELÍASSON AND BJÖRN KARLSSON

Department of Civil and Environmental Engineering, University of Iceland, Hjarðarhagi 6, 107 Reykjavík, Iceland

ANDREJ HORVAT

Intelligent Fluid Solutions Ltd., 127 Crookston Road, London, SE9 1YF, UK

YEHUDA SINAI

HeatAndFlow Consultancy Ltd., 3 Berry Lane, Blewbury, Oxfordshire OX11 9QJ, UK

(Received June 16, 2008)

ABSTRACT: In enclosure fires, density-driven vent flow through an opening to the fire compartment is directly dependent on the state of the fire and the evacuation of smoke and hot gases. If a fire is strongly under-ventilated, there may be heavy production of flammable gases. If a sudden opening occurs, e.g., a window breaks or a fireman opens a door to the fire compartment, fresh air enters the compartment and mixes with hot gases, thus creating a flammable mixture that might ignite and create a backdraft. In this article, we consider the critical flow approach to solve the classical hydraulic equations of density-driven flows in order to determine the gravity controlled inflow in a shipping container full of hot unburnt gases. One-third of the container's height is covered by the horizontal opening. For the initial condition, i.e., just before opening the hatch, zero velocity is prescribed everywhere. When the hatch is opened, the incoming air flows down to the container floor and the hot gas flows out. The interface in between them (the neutral plane) can move up like a free surface in internal flows, making it possible to use the techniques of open channel hydraulics devised by Pedersen [1].

*Author to whom correspondence should be addressed.
E-mail: gjg3@hi.is

0734-9041/10/05 0409–31 $10.00/0 DOI: 10.1177/0734904109354966

In this article the critical flow condition, known from classical hydraulics, is used providing a new equation for the vent flow problem. Two flow correction coefficients are considered at the opening, taking into account the uneven distribution of velocity (α) and the effect of mixing and entrainment (C). The value of these coefficients is evaluated using computational fluid dynamics simulations and physical model results performed for the same geometry. Together, these two coefficients form the flow correction coefficient used in practical formulas for vent flow in fire protection engineering. These are known to have a little different values for different geometries and flow situations. The resulting flow coefficient varies slowly with the density difference, shows a small variation with geometry and compares well with previously published data.

KEY WORDS: critical flow, vent flow, backdraft, gravity currents, CFD.

INTRODUCTION

IF AN ENCLOSED room full of hot unburnt gases is opened, for example, a window breaks or firefighters open a door to the room, fresh oxygen is carried by gravity currents, and mixes with the gases. The dilution of gas with oxygen may create a flammable mixture resulting in ignition and a backdraft gas explosion. This phenomenon is very hazardous and dangerous, and has killed many firefighters in the past years.

Many of the studies and observations concern the plunging density current produced as a cold river enters a warmer lake. The density difference makes the cold water sink under the ambient water, and creates an underflow. Pedersen [1] has published very complete and detailed works on gravity currents, studying and describing in detail the theory of nonmiscible and miscible density driven flows. This theory of density-driven flows has been discussed and applied to a gravity wave entering a flat bottom compartment with full opening [2,3].

Essential problems, such as the state and evolution of the fire or smoke filling and evacuation, depend on the flow through the opening to the fire compartment. Kawagoe [4] suggested the first semi-empirical model for vent flow calculation, assuming a ventilation-controlled fire and a 'well-mixed' condition inside the compartment. Based on the same assumption, Rockett [5] suggested that the inflow was mainly dependent on the shape of the opening rather than on the temperatures. However, several studies have found that his model tends to overestimate the actual vent flow, particularly for large openings. Precise descriptions can be found for various shapes of openings, resulting from experiments [6–8] or from numerical simulations [9].

There are various publications containing formulas for a density-driven flow through an opening. The best known is perhaps from

Emmons [10], also presented in textbooks such as Karlsson et al. [11] and Drysdale [12]. Traditionally, two different flow situations are considered in vent flow calculations: the well-mixed case where the enclosure is considered to have a uniform gas temperature over its entire volume, and the stratified case where the enclosure is only partially filled with hot gases, creating a two-zone model with an upper volume with uniformly distributed gases, and a lower layer of ambient temperature. In both cases, the relationship between the velocity profile and the pressure profile through the vent, obtained with the Bernoulli equation, is used to express the velocity as a function of the height, for both inflow and outflow. In the well-mixed case, the mass flow through the vent depends only on the neutral layer height at the opening, which is determined by equating the volume in and out. On the other hand, in the stratified case, the mass flow rate depends not only on the height of the neutral layer in the opening but also on the hot layer height in the compartment [11, section 5.1.1], leading to a system composed of two unknowns in one equation. Consequently, there is an equation missing in the classical approach so an explicit solution cannot be given in the stratified case [11, section 5.1.1]. In this article we will use a different approach based on the critical flow theory. This theory assumes that the hot fluid flows freely out of the compartment, and consequently passing the obstacle at the top of the vent requires minimum specific energy. This leads to a Froude number equal to one, adding an extra equation to the traditional approach. In the particular case developed in this article, the results obtained using the critical flow theory are similar to the ones obtained with the traditional approach in the well-mixed case. One of the interesting aspects of using the critical flow theory is that it adds an equation to the traditional approach and therefore allows an explicit solution to the vent flow problem. A short description of the theory of critical flow and its application to vent flow is presented in appendix at the end of this article.

The inflow depends on flow coefficients that are due to boundary layer mixing and friction at the interface between the two fluids. Such coefficients have to be extracted from experiments or numerical studies and are often admitted from literature without further research. Fleischmann and McGrattan [13] obtained experimentally very different velocity profiles (Figure 3) than the ones described by the traditional approach. This result was confirmed by numerical simulation. This particular velocity profile justifies the particular effort made in this article to determine the flow coefficients that suit our geometry.

The semi-analytical description of the flow through the opening is then applied to the experiments carried by Gojkovic [14], who conducted a series of 13 experiments using a bigger experimental compartment, but

without measuring the outflow velocities. In order to further evaluate the results from the semi-analytical method, a transient numerical simulation using the ANSYS CFX computational fluid dynamics (CFD) code [15] was conducted to compute the velocity field in Gojkovic's experiments. The transient flow situation showed comparable results in both experiments and computational results so the numerical results for the flow through the opening could be used to extract a flow correction coefficient from it. In the reported simulations, the detached eddy simulation (DES) approach [16] was used to model the flow's turbulent behavior.

Therefore, the geometry and boundary conditions in this article follow the experiments carried by Gojkovic [14], who conducted a series of 13 experiments using methane as fuel, giving a detailed picture of the temperature field during the backdraft.

GEOMETRY OF THE BACKDRAFT EXPERIMENTAL APPARATUS

Fleischmann and McGrattan [13], conducted their experiments using a $2.4 \times 1.2 \times 1.2\,\mathrm{m}^3$ (length $\times$ width $\times$ height) container. Gojkovic [14] used a standard shipping container (Figure 1), measuring $5.5 \times 2.2 \times 2.2\,\mathrm{m}^3$. It was modified in several ways to fulfill its purpose as an experimental apparatus.

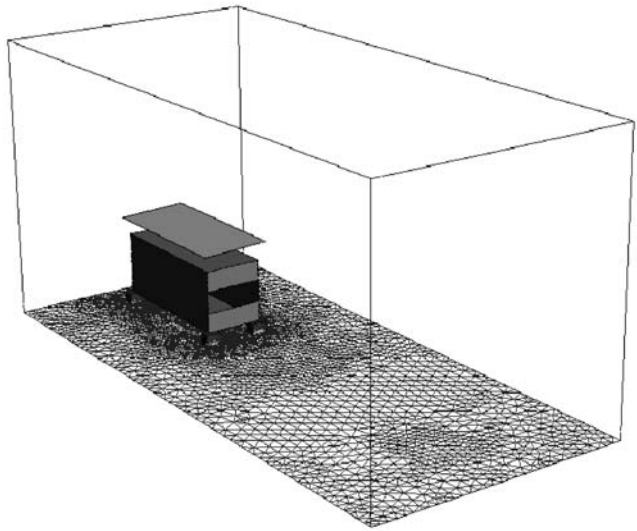

Figure 1. CFD geometry of the backdraft experimental apparatus [14].

In this article, we are particularly interested in the shape of the opening. In Gojkovic, it is vertically centered, 0.8 m high and 1.90 m wide.

FLUID MECHANICAL ANALYSIS

Determination of the Equations of the Inflow and Outflow

A sketch of the opening is shown in Figure 2. In order to determine the inflow velocity, we follow the general theory of density driven flows by Pedersen [1].

The depth-integrated energy equation for the hot layer in the opening is:

$$E_S = P_0 + \rho_h g y + \frac{1}{2}\alpha_h \rho_h V_h^2 = P_0 + \rho_h g y + \frac{1}{2}\alpha_h \rho_h \frac{q_h^2}{(H-y)^2} \qquad (1)$$

where q_h is the flow rate of the hot air flowing out and α is the velocity head factor of classical hydraulics [17] accounting for uneven distribution of velocity in the flow section. This factor equals one when the velocity distribution is even, and this will be discussed in a later section.

We seek a steady state solution for the velocities V_h and V_c that only depends on the density difference, but not on the initial pressure P_0. In the beginning, just after the opening of the hatch, the flow is indeed influenced by the initial pressure conditions as the velocity fluctuations in Figure 6 in [13] clearly show. When steady state is obtained, a difference in static pressures between the inside and the outside

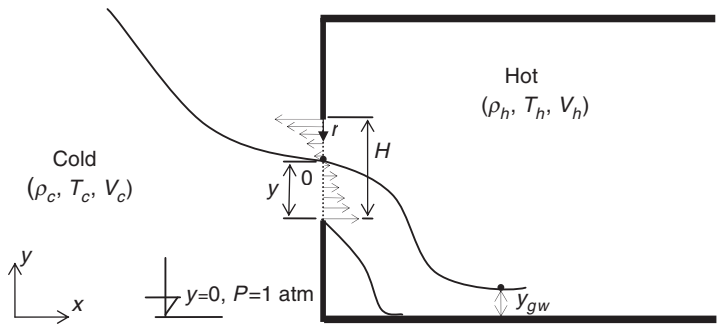

Figure 2. Sketch of the inflow at the opening of the container.

develops so the inflow and outflow will be equal. This requires critical flow (Equation 3.1.6 in [1]) in both layers. In a critical section (not to be mistaken as a section with sonic velocity) the specific energy has a minimum:

$$\frac{\mathrm{d}E_s}{\mathrm{d}y} = \frac{\mathrm{d}P_0}{\mathrm{d}y} + \rho_h g + \alpha_h \rho_h \frac{q_h^2}{(H-y)^3} = 0 \tag{2}$$

Assuming a constant density ρ_c and hydrostatic pressure distribution in the section of opening where the streamlines are almost horizontal, we will have:

$$\frac{\mathrm{d}P_0}{\mathrm{d}y} = \frac{\mathrm{d}}{\mathrm{d}y}(-\rho_c g y) = -\rho_c g \tag{3}$$

Inserting this in Equation (2), we have:

$$\alpha_h \rho_h \frac{q_h^2}{(H-y)^3} = (\rho_c - \rho_h) g \tag{4}$$

This result is similar to a critical flow condition in conventional open channel hydraulics [17].

Pedersen [1] explains that the same formulae apply in density driven flows as in conventional open channel flows just by exchanging the acceleration of gravity g with a reduced acceleration of gravity Δg. Equations (5) and (6) are similar to his results in Δ, with Δ_h for the hot layer and Δ_c for the cold layer. For density differences that are so small that $(1+\Delta)^{-1} \sim 1-\Delta$, these two are equal.

Assuming incompressibility of both flows, the continuity equation leads to $q_h = q_c$, which is equivalent to:

$$\sqrt{\alpha_c}\, y V_c = \sqrt{\alpha_h}(H-y) V_h \tag{5}$$

Equation (5) can be expressed as:

$$\left(\frac{V_h}{V_c}\right)^2 = \left(\frac{y}{H-y}\right)^2 \frac{\alpha_c}{\alpha_h} \tag{6}$$

We can as well combine Equations (5) and (6):

$$\left(\frac{V_h}{V_c}\right)^2 = \frac{H-y}{y} \frac{\alpha_c \rho_c}{\alpha_h \rho_h} \tag{7}$$

Equalizing the Equations (8) and (9), we get:

$$\left(\frac{y}{H-y}\right)^3 = \frac{\rho_c}{\rho_h} \tag{8}$$

We finally obtain the depth of the cold layer:

$$y = \frac{H}{1+(\rho_h/\rho_c)^{1/3}} \tag{9}$$

Here, it is necessary to introduce velocity correction factors C_h and C_h. These correction factor would be equal to one for immiscible frictionless flow, but will in reality be somewhat less than one as mixing slows up the flow. Turbulent mixing between the hot and cold fluid affect the density difference in Equation (4). Now, for the hot layer we obtain:

$$V_h = C_h\sqrt{\frac{\Delta_h g(H-y)}{\alpha_h}} \quad \text{with} \quad \Delta_h = \frac{\rho_c - \rho_h}{\rho_h} \quad \text{and} \quad q_h = V_h(H-y) \tag{10}$$

Similar considerations for the cold layer result in:

$$V_c = C_C\sqrt{\frac{\Delta_c g y}{\alpha_c}} \quad \text{with} \quad \Delta_c = \frac{\rho_C - \rho_h}{\rho_C} \tag{11}$$

The C_h and C_c are empirical correction factors, which are functions of the Reynolds number as discussed in [13] but may also depend on the geometry, especially in fast flows through narrow openings where there is a significant hydrodynamic contraction effect. They are both <1 because the mixing will diminish the average density difference but they do not have to be equal. We will still have $F_\Delta = 1$.

Using Equations (9), (10), and (11), the average velocities V_h and V_c can then be expressed as:

$$V_h = C_h\sqrt{\frac{1}{\alpha_h}\Delta_h g\left(1-\frac{1}{1+(\rho_h/\rho_c)^{1/3}}\right)H} \tag{12}$$

$$V_c = C_c\sqrt{\frac{1}{\alpha_c}\Delta_c g\left(\frac{1}{1+(\rho_h/\rho_c)^{1/3}}\right)H} \tag{13}$$

The Equations (12), (13), and (14), obtained by the critical flow theory, are similar to the ones obtained by Emmons [10] with the traditional approach in the well-mixed case, except for the correction coefficients. These coefficients allow considering the influence of the particular shape of the inflow velocity profile as will be done in the following. It is very different from the one considered in the traditional approach.

Note that the flow regime described above with critical flow condition for both layers is only valid before the filling of the container has reached a certain level. When the depth of the gravity current y_{gw} approaches the level of the neutral plane, we will reach a different flow regime, with the neutral plane moving up. In this second flow regime, only the upper layer will remain critical, and the lower layer will be sub-critical, with velocity $V_c < V_h$. In this article, we assume that backdraft will occur during the primary flow regime. We will not, therefore, describe the second flow regime in detail, but the use of the critical flow theory for this flow situation is described in the appendix as well as the handling of the transient situation when the flow slowly dies down.

Discussion of the Flow Situation and the Correction Factors α and C

The flow correction factors are often included in one general flow coefficient, whose value can typically be between 0.6 and 0.7 for vents and openings [11]. In this section, we will discuss their physical meaning, the flow situation and try to define realistic values for our geometry.

The Flow Situation

When inside the container, the inflow falls down to the floor (Figure 2) and the neutral plane between the hot and the cold air will rise. This will not change the inflow, as changes in back pressure do not change critical flows, until the neutral plane has reached a level sufficiently high to affect the pressure in the critical section in the opening. The inflow will then change to subcritical, slow down and the neutral plane in the opening will rise. The rise can be calculated by equating the rate of change in cold air mass in the compartment to the mass inflow.

These calculations will, however, be difficult. The free fall of the cold air will create quite a splash on the container floor and forced mixing. The mixed air flows across the container floor and forms a hydraulic jump [18] with more mixing that splashes on the back wall and is reflected back. All this happens in a matter of seconds and the density of the resulting mixture in the bottom of the container is difficult to

determine. Nevertheless, the equation for the rate of change of the cold air mass holds so the position of the effective neutral plane (neutral plane position as if there was no mixing), can be determined.

Such calculations will give the time for the rise of the neutral plane up to the opening. This could be a measure of the maximum time from the opening of the hatch until backdraft sets in. When subcritical inflow has set in there is no longer a significant pressure difference between the cold air on the outside and the hot air on the inside, the interface in the opening will continue to rise and the flow discharge will start to diminish as Equation (13) is no longer valid, but Equation (12) still is. Closer description of this transformation from one flow stage to another is in appendix, showing how to handle the stratified case (chapter 5 in [11]) using the critical flow approach.

Significance of the Coefficient α

The coefficient α is defined in [18] as the kinetic energy correction factor of conventional hydraulics, due to uneven distribution of velocity in the opening section. With our notations, Equation (15) in [18] gives:

$$\alpha = \frac{1}{r}\int_{\delta_b}^{H-y}\left(\frac{V}{V_{av}}\right)^3 \mathrm{d}r \tag{14}$$

In [1], the shape of the velocity profile is similar to potential flow in a 180° bend around a wall end. In that situation, the velocity obeys $V \sim 1/r$ (Section 6 in [19]) except at the wall end where a very thin boundary layer will be formed. In this layer the velocity will increase steeply from zero at the wall end to a value V_{max} that will be the beginning of the potential flow profile obeying the $1/r$ law. Now, the velocity profile outside the boundary layer can be modified to $V = A/r + V_{min}$. A is an empirical constant. Figure 3 shows a sketch of this profile and a more precise plot is shown in [13].

With the modified potential flow condition, Equation (14) is:

$$\alpha = \frac{1}{r}\int_{\delta_b}^{H-y}\left(\frac{V}{V_{av}}\right)^3 \mathrm{d}r = \frac{\frac{1}{H-y-\delta_b}\int_{\delta_b}^{H-y}\frac{A^3}{r^3}\,\mathrm{d}r}{\frac{1}{(H-y-\delta_b)^3}\left(\int_{\delta_b}^{H-y}\frac{A}{r}\,\mathrm{d}r\right)^3} = \frac{\frac{(H-y-\delta_b)^2}{2}\left(\frac{1}{\delta_b^2}-\frac{1}{(H-y)^2}\right)}{\left(\ln\left(\frac{H-y}{\delta_b}\right)\right)^3} \tag{15}$$

Observations of values for y and δ from [13], using Equation (15), give us as reasonable estimate for the value of α:

$$\alpha_h = \alpha_c = 1.2$$

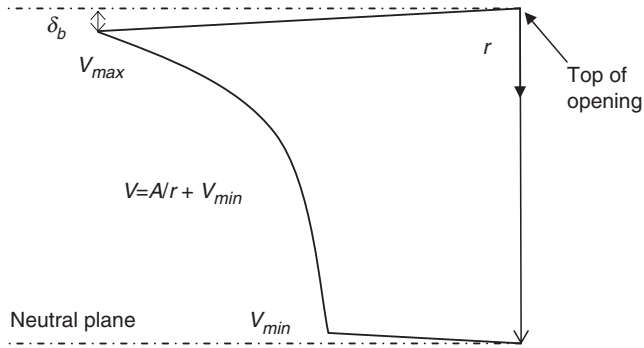

Figure 3. Details of the shape of the outflow.

Significance of the Coefficient C

A detailed qualitative description of the mixing in gravity currents was given by Fleischmann and McGrattan [13], for the experiment as well as for their numerical simulations. Their figures show the importance of the mixed region at the interfacial boundary layer, especially near the opening. We see from the figures the influence of the shape of the opening. Namely, the opening that covers 1/3 of the container's height produces gravity currents with much more mixing than the full opening.

We consider the interface between the two layers, where we have the entrainment velocity V_E [1] and the mixed density ρ_{mix}. Details at the interface are shown in Figure 4.

The continuity equation for the control volume in Figure 4 gives:

$$\rho_h(V_h(H-y)-V_E l_{i,cv})+\rho_c V_E l_{i,cv}=\rho_{mix}V_h l_{o,cv} \tag{16}$$

$$1+\frac{V_E l_{i,cv}}{V_h(H-y)}\Delta_h=\frac{\rho_{mix}}{\rho_h} \tag{17}$$

$$B\frac{V_E}{V_h}\Delta_h=\Delta_{mix} \quad \text{with} \quad \Delta_{mix}=\frac{\rho_{mix}-\rho_h}{\rho_h} \tag{18}$$

We can define the 'true Δ', denoted by Δ_{true}, which takes into account the mixing. $\Delta_{true}=\Delta_h-\Delta_{mix}$.

The critical densimetric Froude number can be written as:

$$F_\Delta=\frac{V_h}{\sqrt{\Delta_{true}g l_{o,cv}}}=1 \tag{19}$$

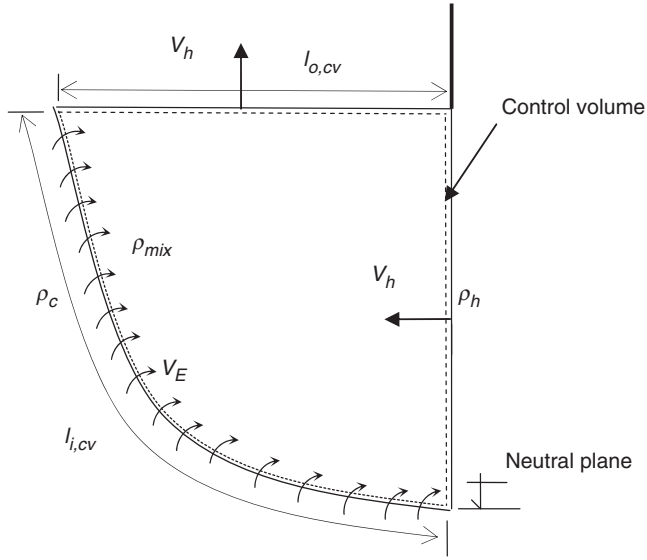

Figure 4. Details of the mixing area at the interface.

$$F_\Delta = \frac{V_h}{\sqrt{\Delta_h g(H-y)}} = \sqrt{\frac{l_{o,cv}}{H-y}}\sqrt{\left(1-\frac{\Delta_{mix}}{\Delta_h}\right)} = C\sqrt{\frac{l_{o,cv}}{H-y}} \tag{20}$$

$$\frac{\Delta_{mix}}{\Delta_h} = B\frac{V_E}{V_h} = 1 - C^2 = f(\Delta) \tag{21}$$

Equation (21) assumes that the relation between the coefficient C and Δ is an unknown function of Δ [1]. For this function we have to find an approximation. For this we will use the results of Fleischmann and McGrattan [13], first the results of their physical experiments, then the results of their numerical simulations for comparison. The two sets of results are in good agreement.

In Fleischmann and McGrattan's experiments the position of the velocity probes is fixed. Therefore, a minor adjustment of the measured average probe velocity values in [13] is needed in order to find the adjusted average velocities in the two layers. This is because the position of the neutral plane y, moves according to Equation (9) and the probes that measure point velocity can only measure average velocity if the position of the probes is moved with the movements of the neutral plane.

The continuity equation at the opening must be fulfilled by the average probe velocities, but with the values reported in [13],

the following inequality is obtained:

$$V_{Sc}y > V_{Sh}(H - y) \tag{22}$$

This does not respect the continuity equation. But if a small correction $\mathrm{d}V$ is applied to the simulated average probe velocities, the following relations are obtained:

$$(V_{Sc} - \mathrm{d}V)y = (V_{Sh} + \mathrm{d}V)(H - y) \tag{23}$$

$$\mathrm{d}V = V_{Sc}y - V_{Sh}(H - y) \tag{24}$$

We finally have our adjusted average velocities of outflow and inflow, noted $V_{h,adj}$ and $V_{c,adj}$:

$$V_{h,true} = V_{Sh} + \mathrm{d}V \tag{25}$$

$$V_{c,true} = V_{Sc} - \mathrm{d}V \tag{26}$$

Figure 5 shows the calculated values of V_h and V_c using Equations (12) and (13) for different values of Δ_h taking into account $\alpha_h = \alpha_c = 1.2$ and $H = 0.4\,\mathrm{m}$ as in [14], the simulated values V_{hs} and V_{cs} extracted from

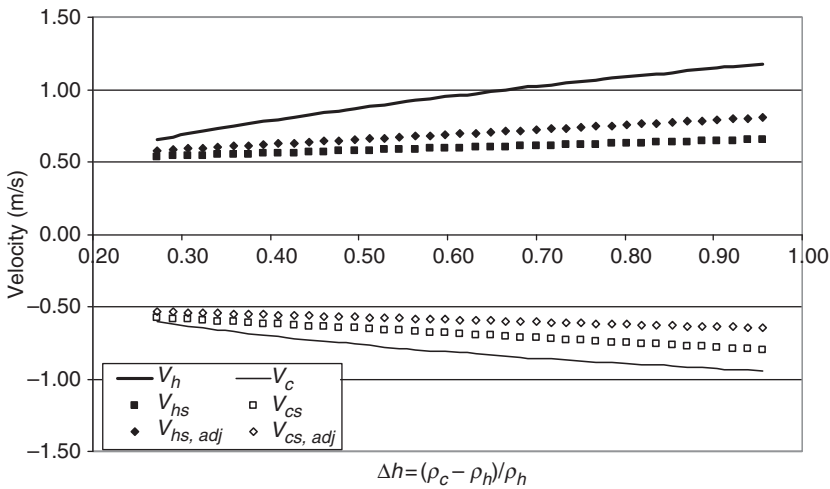

Figure 5. Average velocities at the opening for the Fleischmann–McGrattan geometry (height of the opening = 0.4 m); calculated velocities, simulated (V_{hs} and V_{cs}) and adjusted simulated values ($V_{hs,adj}$ and $V_{cs,adj}$).

Figure 8(b) in [13], and the adjusted velocities $V_{hs,adj}$ and $V_{cs,adj}$ calculated with Equations (25) and (26).

The adjusted velocities allow us to calculate the adjusted coefficient $C_{i,adj} = V_{is,adj}/V_i$. These coefficients are shown in Figure 6. We can note that $C_h \neq C_c$, but $C_{h,adj} = C_{c,adj}$ (the two curves match perfectly). This confirms the necessity to adjust the average probe velocity values, so the continuity equation is respected for all positions of the neutral plane. The function $1 - C_{i,adj}^2$ is also plotted in order to emphasize the variation of $C_{i,adj}$ with Δ. The trendline gives us the function, $f(\Delta)$, which confirms the observation from Equation (21) and shows a very good fit with the emphasized variable $1 - C_{i,adj}^2$.

The function fitted to $C_{h,adj}$ and $C_{c,adj}$ has maximum error = 3.2%. The final result for the flow coefficient is:

$$C_{c,adj} = C_{h,adj} = 0.6641\Delta_h^{-0.1964} \tag{27}$$

This relation is for one geometry only, it will be discussed more closely when comparison of Gojkovics's [14] experiments to the theory presented is discussed.

It should be noted that changes in geometry and all external disturbances of the flow can influence the value of correction coefficient C presented in Figure 6. The coefficient takes into account the velocity retarding effect of the internal fluid friction at the interface caused by

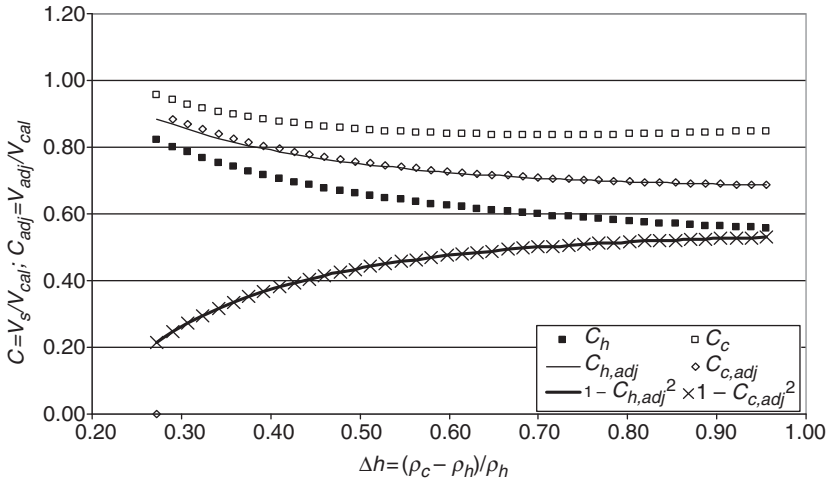

Figure 6. C correction coefficients, calculated coefficients (C_h and C_c), adjusted coefficients ($C_{h,adj}$ and $C_{c,adj}$), ($1 - C_{h,adj}^2$ and $1 - C_{c,adj}^2$) functions and their trendlines.

turbulent mixing. CFD simulations performed in a grid that is fine enough can produce velocities accurate enough so C can be extracted from them. This will be discussed further in the next section.

CFD APPROACH

It is not possible to directly compare the experimental results from Gojkovic's experiments with the theory presented, since no measurements of the velocity fields in the opening were conducted in the experiments. But Horvat et al. [20] have simulated these experiments using Ansys CFX obtaining good agreement with the temperatures observed by Gojkovic. In these simulations we have velocity estimates for a flow situation in the same geometry shown in Figure 2. Here the theory is compared with the velocity fields predicted by Ansys CFX when simulating Gojkovic's experiments.

The approach is based on solving a complete set of transport equations in their discretized form. Due to turbulence and changes in material composition, the Favre-averaged form [16] of transport equations has to be used. Besides the mass and the momentum transport equation for the mixture:

$$\partial_t \rho + \partial_j(\rho \bar{v}_j) = 0 \tag{28}$$

$$\begin{aligned}\partial_t(\rho \bar{v}_i) + \partial_j(\rho \bar{v}_j \bar{v}_i) = &-\partial_i \bar{p} + \partial_j\left(\mu(\partial_i \bar{v}_j + \partial_i \bar{v}_i) - \tfrac{2}{3}\mu(\partial_l \bar{v}_l)\delta_{ji}\right) \\ &+ g(\rho - \rho_{ref}) - \partial_j\left(\rho\overline{v_j' v_i'}\right)\end{aligned} \tag{29}$$

the transport equations for the components CH_4, O_2, H_2O, and CO_2 are needed:

$$\partial_t\left(\rho\bar{\xi}_c\right) + \partial_j\left(\rho\bar{v}_j\bar{\xi}_c\right) = \partial_j\left(\rho D_c \partial_j \bar{\xi}_c\right) - \partial_j\left(\rho\overline{v_j'\xi_c'}\right) \tag{30}$$

Furthermore, the energy equation was written for the total specific enthalpy:

$$\partial_t\left(\rho\bar{h}_{tot}\right) - \partial_t p + \partial_j\left(\rho\bar{v}_j\bar{h}_{tot}\right) = \partial_j\left(\lambda\partial_j\bar{T}\right) - \partial_j\left(\rho\overline{v_j' h_{tot}'}\right) \tag{31}$$

In the present work, the CFX version of the DES model [15] was used to model turbulence. Using the large eddy simulation (LES) turbulence model to resolve flow structures in wall boundary layer flows at high Re numbers requires fine grid resolution, which is computationally

extremely expensive, and therefore not useful for most industrial flow simulations. The DES model is an attempt to combine elements of RANS and LES formulations into a hybrid formulation, where Menter's shear stress transport (SST) model is used inside attached and mildly separated boundary layers, and the LES model is applied in massively separated regions. To distinguish these two regions, a turbulence length scale, calculated as [21,22]:

$$l_{RANS} = \frac{\sqrt{k}}{C_\mu \omega} \tag{32}$$

is compared with a length scale associated with the local grid spacing δ and the LES model:

$$l_{LES} = C_{DES}\delta \tag{33}$$

The DES model switches from the SST model to the LES model in the regions where the turbulence length scale l_{RANS} is larger than the local LES model scale l_{LES}.

Turbulent viscosity is defined as in the SST model as a ratio between turbulence kinetic energy k and eddy frequency ω:

$$\mu_t = \frac{a_1 k}{\max(a_1\omega, F_2 S)} \tag{34}$$

Turbulence heat and mass fluxes are then calculated as:

$$\rho\overline{v_j' h_{tot}'} = -\frac{\mu_t}{Pr_t}\partial_j \bar{h} \quad \text{and} \quad \rho\overline{v_j'\xi'} = -\frac{\mu_t}{Sc_t}\partial_j \bar{\xi} \tag{35}$$

Usually, the molecular mass diffusivity ρD_c is small compared to the turbulence mass diffusivity μ_t/Sc_t and is often unknown.

Initially, the container is filled with a mixture that contains methane, air and combustion products. Gojkovic [14] reported the total amount of methane that was released into the compartment. The fuel inventory was partially reduced due to initial burning, and the resulting composition of the mixture was rich in unburned methane and combustion products with a relatively small amount of oxygen that is unable to support burning. In view of the uncertainties, the following initial content was assumed in the model for all simulated cases:

$$\begin{aligned} &\overline{\Psi}_{CH_4} = 0.22, \quad \overline{\Psi}_{CO_2} = 0.02 \\ &\overline{\Psi}_{H_2O} = 0.04, \quad \overline{\Psi}_{O_2} = 0.1196, \quad \overline{\Psi}_{N_2} = 0.6004 \end{aligned} \tag{36}$$

The initial velocity was set to 0.0. Temperature inside the container was varied to obtain a desirable value of Δ_h. Therefore, T_h was 37.5°C for $\Delta_h = 0.2$, 75°C for $\Delta_h = 0.4$, 125°C for $\Delta_h = 0.6$, and 175°C for $\Delta_h = 0.8$.

For the external initial composition, we assumed fresh air:

$$\overline{\Psi}_{CH_4} = 0.0, \quad \overline{\Psi}_{O_2} = 0.21, \quad \overline{\Psi}_{N_2} = 0.79, \quad \overline{\Psi}_{CO_2} = 0.0, \quad \overline{\Psi}_{H_2O} = 0.0 \quad (37)$$

and an initial temperature of 5°C in all cases.

For the simulations' boundary conditions, the no-slip, smooth, adiabatic boundary conditions were set for all walls. At the outermost boundaries of the domain, wall conditions were set at the floor and pressure conditions (openings) at the remaining boundaries, with an ambient temperature of 5°C. At openings, flow may enter or leave, depending on the local pressure just inside the boundary.

The ANSYS CFX software [15] was used to set up the gravity current model and to solve the transport equations for mass (28), momentum (29), species (30), total enthalpy (31), turbulence kinetic energy, and eddy frequency, with the described initial and boundary conditions.

APPLICATION TO GOJKOVIC'S EXPERIMENTAL COMPARTMENT – COMPARISON BETWEEN SEMI-ANALYTICAL AND THE CFX NUMERICAL RESULTS

We have, in the previous part, defined the equations of the outflow (12) and inflow (13) at the opening of the container as well as the position of the neutral plane. The equations and flow correction coefficients can now be adapted to the experimental container. Figure 7 shows the velocities computed semi-analytically, as well as the results of the numerical simulations performed with the ANSYS CFX code. A 3D numerical mesh with 162,552 nodes and 862,811 elements was generated to perform the numerical analysis. The average mesh spacing inside the enclosure was 5 cm. The initial time step was set to $dt = 0.005$ of the gravity wave timescale $L/\sqrt{\Delta_h g H}$. Four different cases were simulated with $\Delta_h = 0.2$, 0.4, 0.6, and 0.8, respectively.

Figure 8 shows the height of the neutral plane for both the semi-analytical and the numerical calculations.

Analysis of the Results

In Figure 7, the velocities from the CFX simulations are compared to the theory using Equation (27) for C. Furthermore Figure 8 shows the

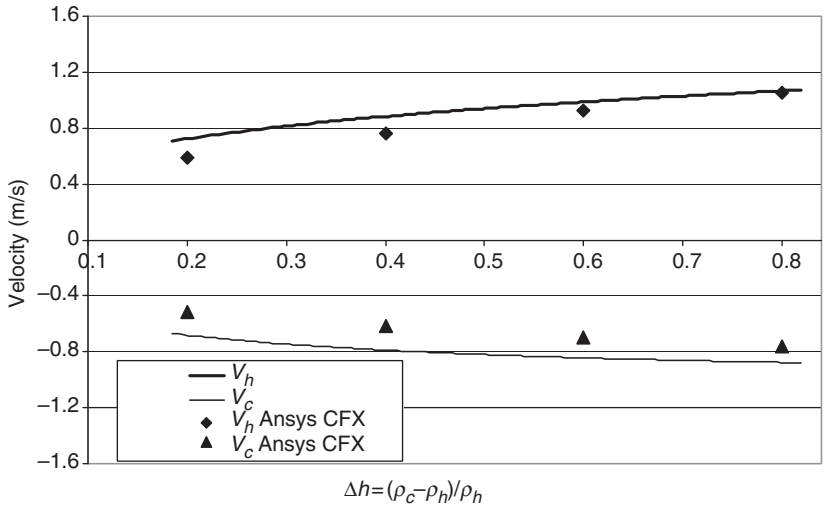

Figure 7. Average velocities at the opening for the Gojkovic experimental apparatus (height of the opening = 0.8 m) using correction coefficients from Equation (27).

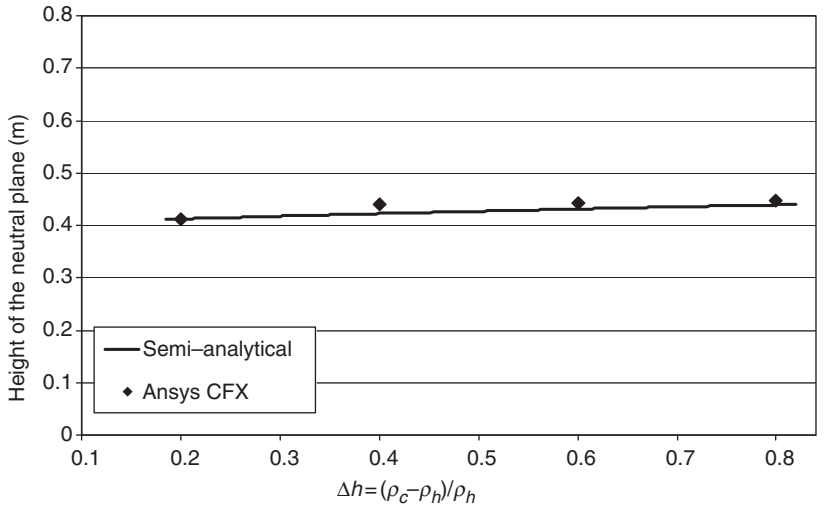

Figure 8. Height of the neutral plane at the opening for the Gojkovic experimental apparatus (height of the opening = 0.8 m).

Table 1. Flow characteristics at the opening for the Gojkovic experimental apparatus (height of the opening = 0.8); comparison between semi-analytical and numerical results.

	Correction fact		V_h (m/s)		V_c (m/s)		Q (m^3/s)	Q_h (m^3/s)	Q_c (m^3/s)	Y (m)	
Δ_h	α	C	analyt	simul	analyt	simul	analyt	simul	simul	analyt	simul
0.2	1.2	0.905	0.729	0.588	−0.685	−0.518	0.537	0.501	0.469	0.412	0.413
0.4	1.2	0.793	0.884	0.760	−0.790	−0.611	0.634	0.601	−0.591	0.423	0.441
0.6	1.2	0.734	0.987	0.929	−0.844	−0.697	0.691	0.731	−0.677	0.431	0.442
0.8	1.2	0.694	1.065	1.057	−0.876	−0.761	0.731	0.821	−0.747	0.439	0.447

Note that the CFD results are averaged over a time period between 1.2 and 6.8 s after door opening, when the flow is stabilized after the initial phenomena.

Table 2. Difference ratio between analytical and simulated flow characteristics at the opening for the Gojkovic experimental apparatus (height of the opening = 0.8).

Δ_h	R (V_h) %	R (V_c) %	R (Q_h) %	R (Q_c) %	R (Y) %
0.2	19.35	24.46	6.77	12.68	0.03
0.4	14.10	22.64	5.26	6.74	4.31
0.6	5.92	17.35	5.75	2.04	2.54
0.8	0.77	13.10	12.43	2.25	1.78

height of the neutral plane at the opening for the Gojkovic experiment. Then the numerical results are presented in Table 1. The results compare favorably but the difference is one sided.

The comparison given in Figures 7 and 8 as well as in Table 1, show a good agreement between the semi-analytical and the simulated values when Equation (27) is used for the correction coefficient. We can now define a difference ratio R for a value X as:

$$R(X) = \left| \frac{X_{analyt} - X_{simul}}{X_{analyt}} \right| \% \tag{38}$$

In Table 2, the difference ratios for the uncorrected values of velocities and flows are presented for the range of density ratios covered by the data referred.

Most of the cases show 5–20% difference between the results of the semi-analytical procedure and the CFD simulations when Equation (27) is used. This difference drops to under 5% when the following

Equation (39) is used as the correction coefficient for the Gojkovic experiment:

$$C_{c,adj} = C_{h,adj} = 0.6229\Delta_h^{-0.0741} \tag{39}$$

The correction factor Equation (27) is calculated from the results of Fleischmann and McGrattan [13]. Comparison of Equations (27) and (39) shows an average difference of 15% between them in the density difference range covered by the data in Table 2. This is a small difference considering the large differences in geometry and size between the two experimental setups of Fleischmann and McGrattan on one side and Gojkovic on the other side. Then there are other sources of inaccuracy already described. We find the simulation of the Gojkovic experiment closer to actual fire situations, therefore it is concluded more appropriate to use Equation (39) in problems of this type. In the case when results accurate within the 15% limit are needed a full CFD investigation in a fine grid model must be recommended.

PRACTICAL FORMULAS

Using Equations (9), (11), (13), and (39) gives a formula for the mass flow through vents with a critical section:

$$\dot{m} = \rho_c q = CyB\sqrt{\rho_c(\rho_c - \rho_h)gy} \tag{40}$$

The dimension is kg/s in SI units. B is width of the opening.

The variable y is:

$$y = \frac{H}{1 + (\rho_h/\rho_c)^{1/3}}$$

The flow coefficient C is.

$$C = 0.57\left(\frac{\rho_c - \rho_h}{\rho_h}\right)^{-0.0741}$$

Equation (40) can be compared to the well-known simple formula Equation 5.24 in [11]. If we take a practical example: $\rho_c = 1{,}2\,\text{kg/m}^3$, $\rho_h = 0{,}616\,\text{kg/m}^3$, and $H = 2\,\text{m}$, Equation (40) gives the flow $1.76\,\text{kg/m}^3$ while Equation 5.24 in [11] gives $1.41\,\text{kg/m}^3$. The difference is 24%.

CONCLUSIONS

In this article, we discuss a semi-analytical approach, which calculates the characteristics of the steady-state flow created by density difference at the opening of a container full of hot gases. In a stratified case, solving vent flow equations by application of the Bernoulli principle leads to two unknowns, the height of the neutral plane and height of the hot layer, which does not allow an analytical solution of the problem. This new approach, based on the critical flow condition, overcomes this and allows direct calculation of the flow through the vent with a relatively simple equation.

The new flow equations include empirical flow coefficients like existing formulas in fire protection engineering do. To find the coefficients, we used the results of one series of physical experiments, CFD simulated results for a small container, and another simulation, this time the Gojkovic's backdraft experiments simulated by Horvat using the ANSYS CFX software. The resulting flow coefficients compare very well, difference in sizes of compartment and different geometries taken into account.

It also confirms that correction factors calculated for one geometry cannot readily be applied to another geometry if accurate results are required. In practical calculations the new vent flow formula is very handy and gives results not far from what simple formulas, popular in practical fire protection engineering give.

The behavior of the gravity wave inside the container under the influence of forced mixing and hydraulic jumps is currently being studied by a number of workers in the field. The results presented in this article, with the description of the opening flow characteristics, are therefore important for this research project on under-ventilated fires.

APPENDIX: APPLICATION OF CRITICAL FLOW CONDITIONS TO VENT FLOW

Generality on Specific Energy and Critical Flow

The concept of specific energy and critical flow has been developed to study open channel flow [17]. The specific energy of a channel flow of depth y is:

$$E = y + \frac{V^2}{2g} \tag{A1}$$

In the case of a rectangular channel, considering the discharge per unit width $q = Q/b = V{\cdot}y$, the specific energy is:

$$E = y + \frac{q^2}{2gy^2} \tag{A2}$$

This energy is minimum for $\mathrm{d}E/\mathrm{d}y = 0$, referred as the critical flow condition, and the corresponding depth called the critical depth y_{cr}.

$$\frac{\mathrm{d}E}{\mathrm{d}y} = 0 = 1 - \frac{q^2}{gy_{cr}^3} \tag{A3}$$

$$y_{cr} = \left(\frac{q^2}{g}\right)^{\frac{1}{3}} \tag{A4}$$

$$q^2 = gy_{cr}^3 = (gy_{cr})y_{cr}^2 = V_{cr}^2 y_{cr}^2 \tag{A5}$$

The former equation can finally be expressed as the Froude number:

$$Fr = \frac{V_c}{\sqrt{gy_{cr}}} = 1 \tag{A6}$$

The evolution of the specific energy is shown on Figure A1.

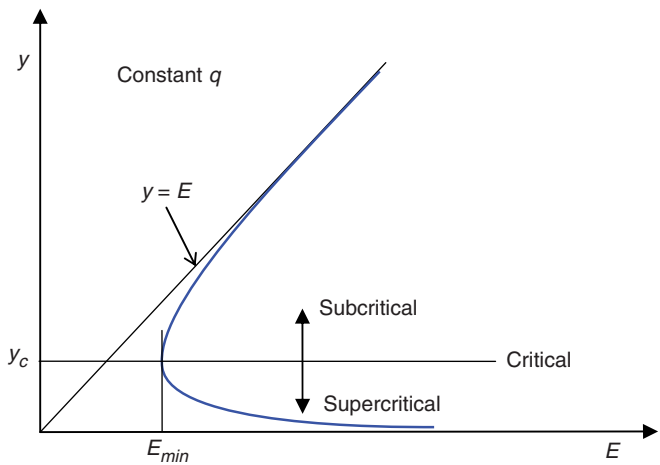

Figure A1. Specific energy E vs depth y. E is minimum at critical depth y_c.

For $E < E_{min}$, there are no solutions, and thus such a flow is physically impossible.

For $E < E_{min}$, there are two possible solutions:

Subcritical flow at large depth with $V < V_c$. In this case, $Fr < 1$.
Supercritical flow at small depth with $V > V_c$. In this case, $Fr > 1$.

For $E = E_{min}$, the flow is critical and $Fr = 1$. This corresponds to an equilibrium state where the flow requires minimum specific energy to pass over an obstacle.

Application to Density Driven Flows in Fire Safety Engineering

A vent flow through an opening into a fire compartment or gravity waves are density driven flows. This problem has been studied extensively by Pedersen [1], where he demonstrates that the conventional equations of open channel flow can be applied to density driven flow, by exchanging the acceleration of gravity g with a reduced acceleration of gravity Δg. Δ is called the dimensionless reduced mass defined as: $\Delta_c = (\rho_c - \rho_h)/\rho_c$.

The densimetric Froude number characterizing a density driven flow is therefore:

$$Fr_\Delta = \frac{V}{\sqrt{\Delta g y}} \tag{A7}$$

This obeys the same rules for critical flow in an open channel described above. The concept of reduced acceleration of gravity and its application to gravity wave in potential backdraft condition is described and discussed in [2].

The densimetric Froude approach is particularly interesting to describe the flow through a vent opening. In fire safety engineering, the most widely used calculation methods are based on the Bernoulli equation of the flow [10,11]. In these textbooks, there are a few references to literature in hydraulic science. Since they appeared there has been an important progress in hydrodynamics and hydraulics, especially in stratified flows that has not found its way into vent flow formulas available to fire safety engineers. In well-mixed case, the inflows and outflows can be calculated using only the Bernoulli approach. In stratified flows, this approach leads to two unknowns, the height of the neutral plane and the depth of the hot layer inside the

compartment, which does not allow an analytical solution. This problem is solved by applying the critical flow condition.

Well-mixed Case

The following Equations (A8) and (A9) are presented widely in the literature, and correspond for example to Equations (5.18) and (5.19) in [11]. The mass flow of the hot and cold fluid are integrated over y_h and $(H - y_h)$, respectively.

$$q_h = \frac{2}{3} C_d \sqrt{\frac{2g\Delta_h}{\alpha}} y_h^{\frac{3}{2}} \tag{A8}$$

$$q_c = \frac{2}{3} C_d \sqrt{\frac{2g\Delta_h}{\alpha}} y_c^{\frac{3}{2}} = \frac{2}{3} C_d \sqrt{\frac{2g\Delta_h}{\alpha}} (H - y_h)^{\frac{3}{2}} \tag{A9}$$

where C_d is a flow correction factor between 0.6 and 0.7. α is added to consider the uneven distribution of velocities.

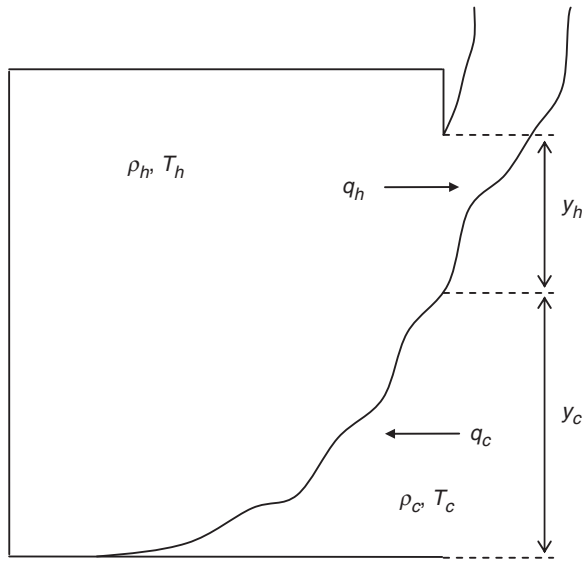

Figure A2. Sketch of the flow through a compartment vent in the well-mixed case.

The height of the neutral plane is determined by considering the conservation of mass and thus equalizing the mass flow rates in and out. The flow rates can then be calculated.

Stratified Flows

In stratified flows, there is formation of a hot layer under the ceiling. The problem arises because the height of the neutral plane is different from the height of this hot layer, with a mixed zone between the layers, thus adding an extra unknown to the set of Equations (A8) and (A9).

Applying the theory of critical flow can overcome this problem. The hot fluid flows freely out of the compartment, pushed by the gravity difference. Passing the obstacle at the top of the vent requires minimum specific energy. The depth of the hot layer is consequently critical at the opening and the critical Froude number is:

$$Fr_{\Delta} = \frac{V_{cr}}{\sqrt{\frac{\Delta g y_{cr}}{\alpha}}} = \frac{V_h}{\sqrt{\frac{\Delta g y_h}{\alpha}}} = 1 \qquad \text{(A10)}$$

When the y_{mix} is much smaller than the total height of the hot zone $h = y_h + y_{mix}$ we have $h - y_h = y_h/2 = y_{mix}$ and we can calculate the flow in terms of h.

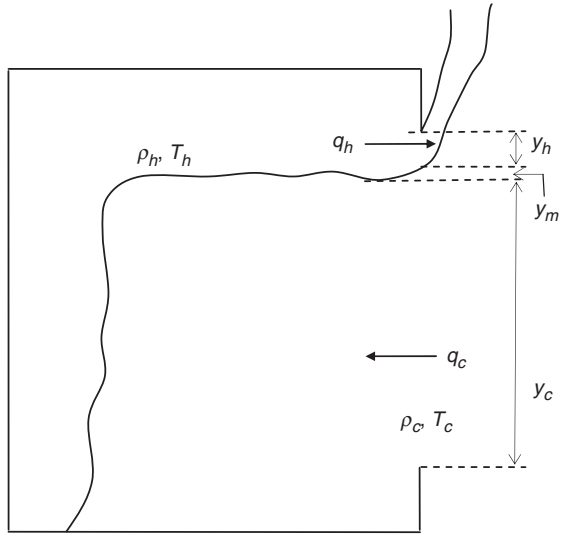

Figure A3. Sketch of the flow through a compartment vent in the stratified case.

This gives the following flow rate:

$$q_h = C_Q y_h \sqrt{\frac{\Delta_h g y_h}{\alpha}} = C_Q \frac{2}{3} h \sqrt{\frac{2}{3}} \sqrt{\frac{\Delta_h g h}{\alpha}} = 0.45 h \sqrt{\Delta_h g h} \qquad \text{(A11)}$$

The coefficient C_Q is generally between 0.9 and 0.94. The value 0.9 has been used to obtain the last expression. A complete discussion about loss coefficients for different flows is in [17]. Equation A11 can also be used when the outflow is known (e.g., the smoke emission from a fire in the compartment) to calculate the height of the hot zone (thickness of the ceiling layer of hot gas). The transient (unsteady) situation, i.e., the build up of a layer or the reduction of it, can also be calculated using the continuity (mass balance) equation for the total volume of hot gas. The increase in total volume of hot gas in the compartment is the difference between gas produced and gas flowing out.

$$\frac{\mathrm{d}M_{tot}}{\mathrm{d}t} = A \frac{\mathrm{d}h}{\mathrm{d}t} = \dot{M}_G - q_h = \dot{M}_G - 0.45 h \sqrt{\Delta_h g h} \qquad \text{(A12)}$$

Here A is the compartment area and M_G the hot gas production rate of the fire. Equation (A12) cannot be readily integrated, but numerical integration is no problem. One will find that it takes surprisingly long time for h to reach the equilibrium value h_0 when the outflow equals the production rate in big compartments. Mistaking a transient situation for an equilibrium one can result in serious errors in gas flow and layer height estimations.

NOMENCLATURE

a_1 = SST model coefficient, equal to 0.31
A = Empirical constant
B = Empirical constant
C = Velocity correction factor
C_c = Velocity correction factor for the cold layer
C_h = Velocity correction factor for the hot layer
C_{DES} = Turbulence model coefficient, equal to 0.61
C_μ = Turbulence model coefficient, equal to 0.09
$C_{c,adj}$ = Adjusted velocity correction factor for the cold layer
$C_{h,adj}$ = Adjusted velocity correction factor for the hot layer
$C_{i,adj}$ = Adjusted velocity correction factor for the layer i
D_c = Kinematic mass diffusivity
$\mathrm{d}t$ = Initial time step

dV = Velocity correction
E_S = Depth integrated energy
F_2 = SST model function
F_Δ = Densimetric Froude number
g = Acceleration of gravity
H = Height of the opening
h_{tot} = Total enthalpy
k = Turbulent kinetic energy
L = Length of the container
l = Turbulence length scale
l_{LES} = Turbulence length scale for the Large-Eddy Simulation model
l_{RANS} = Turbulence length scale for the Reynolds Averaged Navier-Stokes model
$l_{i,cv}$ = Length of the interface at the control volume
$l_{o,cv}$ = Length of the flow out of the control volume
P_0 = Pressure at the neutral plane
Pr_t = Turbulent Prandtl number, equal to 0.9
p = Pressure
Q_c = Volumetric flow rate of the cold layer
Q_h = Volumetric flow rate of the hot layer
q_c = Flow rate of the cold layer per unit width
q_h = Flow rate of the hot layer per unit width
R = Difference ratio between analytical and simulated results
Re = Reynolds number
r = Distance to the top of the opening for potential theory
S = Invariant measure of the strain rate
Sc_t = Turbulent Schmidt number, equal to 0.9
T = Temperature
T_c = Temperature of the cold layer
T_h = Temperature of the hot layer
t = Time, time scale
V = Velocity for potential flow profile
V_{av} = Average velocity at the opening
V_c = Average velocity of the cold layer at the opening
V_E = Velocity entrainment at the interface
V_h = Average velocity of the hot layer at the opening
V_i = Average velocity of the layer i at the opening
V_{max} = Maximum velocity for potential flow profile
V_{min} = Minimum velocity for potential flow profile
V_{cs} = Simulated average velocity of the cold layer at the opening
V_{hs} = Simulated average velocity of the hot layer at the opening
V_{is} = Simulated average velocity of the layer i at the opening

$V_{cs,adj}$ = Adjusted simulated average velocity of the cold layer at the opening
$V_{hs,adj}$ = Adjusted simulated average velocity of the hot layer at the opening
$V_{is,adj}$ = Adjusted simulated average velocity of the hot layer i at the opening
$V_{c,true}$ = True average velocity of the cold layer at the opening
$V_{h,true}$ = True average velocity of the hot layer at the opening
W = Width of the container
W_{op} = Width of the opening
X_{analyt} = Analytical value of a function X
X_{simul} = Simulated value of a function X
x = Spatial coordinate
y = Height of the cold layer at the opening
y_{gw} = Height of the gravity wave

GREEK LETTERS

α = Velocity head factor
α_c = Velocity head factor of the cold layer
α_h = Velocity head factor of the hot layer
δ = Grid spacing
δ_b = Thickness of the boundary layer
δ_{ij} = Kronecker delta function
Δ = Dimensionless reduced mass function
Δ_c = Dimensionless reduced mass, $\Delta_c = (\rho_c - \rho_h)/\rho_c$
Δ_h = Dimensionless reduced mass, $\Delta_h = (\rho_c - \rho_h)/\rho_h$
Δ_{mix} = Dimensionless reduced mass, $\Delta_{mix} = (\rho_{mix} - \rho_h)/\rho_h$
Δ_{true} = True dimensionless reduced mass
λ = Wave length, eigenvalues
μ = Dynamic viscosity
μ_t = Eddy viscosity
ν_j = Velocity (component j)
ξ_c = Mass fraction of component c
ρ = Density
ρ_h = Density of the hot layer
ρ_c = Density of the cold layer
ρ_{mix} = Mixed density at the interface
ρ_{ref} = Density at reference state (for CFD model)
Ψ = Volume fraction
ω = Eddy frequency

SYMBOLS

$\overline{\ }$ = Turbulence model time averaged value
$'$ = Turbulence model fluctuating component
∂_j = Partial derivative in j-direction

REFERENCES

1. Pedersen, F.B. (1986). *Environmental Hydraulics: Stratified Flows*, Springer Verlag, Berlin Heidelberg.
2. Elíasson, J., Guigay, G. and Karlsson, B. (2008). Enclosure Fires, Gravity Currents and the Backdraft Problem, *Journal of Fire Sciences*, **26**: 373–397.
3. Guigay, G. (1998). A CFD and Experimental Investigation of Under-ventilated Compartment Fires, PhD Thesis, Department of Civil and Environmental Engineering, University of Iceland. Available at: http://www.skemman.is//handle/1946/3439
4. Kawagoe, K. (1958). *Fire Behaviour in Rooms*, Report No. 27, pp. 1–72, Building Research Institute, Japan.
5. Rockett, J. (1976). Fire Induced Gas Flow in an Enclosure, *Combustion Science and Technology*, **12**: 165–175.
6. Steckler, K.D., Quintiere, J.G. and Rinkinen, W.J. (1982). Flow Induced by Fire in a Compartment. US Department of Commerce, NBSIR 82-2520.
7. Thomas, P.H., Heselden, A.J.M. and Law, M. (1967). Fully-developed Compartment Fires – Two Kinds of Behaviour, Fire Research Technical Paper No. 18, Ministry of Technology and Fire Offices' Committee, Joint Fire Research Organisation, HMSO, UK, pp. 2–5.
8. Babrauskas, V. and Williamson, R.B. (1978). Post-flashover Compartment Fires: Basis of a Theoretical Model, *Fire and Materials*, **2**(2): 39–53.
9. Chow, W.K. and Zou, G.W. (2004). Correlation Equations on Fire-induced Air Flow Rate through Doorway Derived by Large Eddy Simulation, *Building and Environment*, **40**(7): 897–906.
10. Emmons, H.W. (1995). Vent Flows, In: National Fire Protection Association (ed.), *The SFPE Handbook of Fire Protection Engineering*, Section 2, Chapter 5, **2nd edn**, National Fire Protection Association, Quincy, Massachusetts.
11. Karlsson, B. and Quintiere, J.G. (1986). *Enclosure Fire Dynamics*. CRC Press, Boca Raton.
12. Drysdale, D. (1998). *An Introduction to Fire Dynamics*, **2nd edn**, John Wiley and Sons, Chichester.
13. Fleischmann, C.M. and McGrattan, K.B. (1999). Numerical and Experimental Gravity Currents Related to Backdrafts, *Fire Safety Journal*, **33**: 21–34.
14. Gojkovic, D. (2000). *Initial Backdraft Experiments*, Department of Fire Safety Engineering, Lund University, Sweden.
15. ANSYS CFX. Available at: http://www.ansys.com/products/cfx.asp and online documentation, http://www-waterloo.ansys.com/community/

16. Menter, F.R. and Kuntz, M. Development and Application of a Zonal DES Turbulence Model for CFX-5, CFX-Validation Report, CFX-VAL17/0503.
17. Titus, J.J. (1995). Hydraulics, In: National Fire Protection Association (ed.), *The SFPE Handbook of Fire Protection Engineering*, Section 4, Chapter 2, **2nd edn**, National Fire Protection Association, Quincy, Massachusetts.
18. White, F.M. (1999). *Fluid Mechanics*, **4th edn**, WCB McGraw-Hill, New York.
19. Olson, R.M. and Wright, S.J. (1990). *Essential of Engineering Fluid Mechanics*, **5th edn**, Harper and Row Publishers Inc., New York.
20. Horvat, A., Sinai, Y., Gojkovic, D. and Karlsson, B. (2008). Numerical and Experimental Investigation of Backdraft, *Combustion Science and Technology*, **180**(1): 21–34.
21. Menter, F.R. (1994). Two-equation Eddy-viscosity Turbulence Models for Engineering Applications, *AIAA Journal*, **32**(8): 1598–1605.
22. Menter, F.R., Kunz, M. and Langtry, R. (2003). Ten Years of Industrial Experience with the SST Turbulence Model, In: Hanjalic, K., Nagano, Y. and Tummers, M. (eds), *Turbulence, Heat and Mass Transfer 4*, pp. 625–632, Begell House, New York.

BIOGRAPHIES

Georges Guigay

Georges Guigay studied at the Joseph Fourier University in Grenoble, France, where he gained a BSc degree in Mechanical Engineering in 1996 and a MSc degree in Numerical Simulation in 1998, specializing in Computational Fluid Dynamics. From 1998 to 2004, he worked as a researcher and a consulting engineer in both France and Iceland. In 2004, he joined a PhD program at the University of Iceland, focusing his research on underventilated fires and smoke gas explosions, such as backdraft. He defended his PhD thesis in September 2008. He is currently working as a Fire Safety Engineer for Mannvit Engineering in Iceland, and as a part-time teacher and researcher at the University of Iceland.

Jónas Elíasson

Jónas Elíasson was born on May 26, 1938 in Iceland, got his Civil Engineering degree (MSc) from the Technical University of Denmark in 1962 and PhD from the same University in 1973. After various engineering assignments he was professor of hydraulics, hydrology and coastal engineering at the University of Iceland 1973–2008. He has held numerous appointments e.g., as Chairman of the Board of Jarðboranir h.f. (Icelandic Drilling Co.) 1987–1990 and 1991–2000, Deputy Minister of Industry 1985–1987, Chairman of the Board, National Energy

Authority 1985–1988 and Harbour of Reykjavik, Board Member 1982–1995, vice chairman 1986–1995. He has written numerous scientific papers and articles in professional journals and elsewhere.

Björn Karlsson

Björn Karlsson graduated in Civil Engineering (Hons) from Heriot-Watt University, Edinburgh 1986, acquired his Licentiate from the Department of Fire Safety Engineering at Lund University, Sweden in 1989 and received a PhD degree from the same department in 1992. He worked as Associate Professor at the department from 1993 to 2001, was a Visiting Professor at the University of Maryland 1996, and became Fire Marshal and General Director of the state run Iceland Fire Authority, Reykjavik, Iceland in 2001. Björn is an Associate Professor at the Department of Environmental and Civil Engineering at the University of Iceland.

Andrej Horvat

Andrej is a Principal Engineer at Intelligent Fluid Solutions (IFS), an engineering company that provides R&D, engineering analysis and design services in the area of fluid mechanics, heat and mass transfer. His responsibilities are technical group support, project management and consumer products development. Prior to his current appointment, Andrej worked as a technical consultant for ANSYS Europe and as research associate for Reactor Engineering Division of Josef Stefan Institute. Andrej received Dipl. -Ing. degree in Process Engineering at University of Maribor, MSc in Nucl. Eng. at University of Ljubljana, PhD in Nucl. Eng. at University of Ljubljana and MSc in Mech. Eng. at University of California, Los Angeles. Since then he published more than 20 journal papers on different aspects of fluid dynamics and heat transfer.

Yehuda Sinai

Yehuda Sinai qualified in mechanical engineering at Witwatersrand University (South Africa) in 1968. In 1969 he won a Cessna 150 aeroplane in a flying competition, and later travelled to the UK, where he obtained a PhD at Cranfield in 1975, on non-equilibrium molecular relaxation effects in sonic booms. After a spell in academe working on acoustics and two-phase fluid-structure vibrations, he spent 10 years at NNC, principally on mathematical modeling of nuclear safety thermal-hydraulics. He joined AEA Technology in 1992, where he specialized in

CFD modeling in the safety sphere, and became CFD Project Manager for Fire, Safety, HVAC and Environment. This role continued after the acquisition of AEA's CFD operation by ANSYS Inc. in 2003. In July 2009 Yehuda left ANSYS and set up his own company named HeatAndFlow Consultancy Ltd., offering general modeling and project management.